Thermodynamic Studies on Order-Disorder Phase Transitions of *p*-Terphenyl and *p*-Terphenyl-d_{14}†

Kazuya SAITO,†† Tooru ATAKE,††† and Hideaki CHIHARA*
Department of Chemistry and Chemical Thermodynamics Laboratory, Faculty of Science, Osaka University, Toyonaka, Osaka 560
††Department of Chemistry, Faculty of Science, Tokyo Metropolitan University, Fukazawa, Setagaya-ku, Tokyo 158
†††Research Laboratory of Engineering Materials, Tokyo Institute of Technology, 4259 Nagatsuta-cho, Midori-ku, Yokohama 227
(Received January 30, 1988)

The heat capacities of *p*-terphenyl and *p*-terphenyl-d_{14} were measured by adiabatic calorimetry between 3 and 300 K. The phase transition associated with a molecular conformation change was observed as a λ-shaped anomaly at (193.5±0.1) K and at (180.3±0.1) K. The enthalpies of transition are (304±20) J mol^{-1} and (288±20) J mol^{-1} and the entropies of transition are (1.63±0.10) J K^{-1} mol^{-1} and (1.63±0.10) J K^{-1} mol^{-1}, respectively. The anisotropy of the intermolecular interaction is discussed and the anomalous portion of the heat capacities in the transition region was compared favorably with a two-dimensional Ising model.

The molecule of *p*-terphenyl (1,1′:4′,1″-terphenyl) is twisted in the gaseous and in the liquid states.[1-4] However, it is seemingly planar in the crystal at room temperature.[5-8] The crystal belongs to the space group $P2_1/a$ and the molecule occupies the center of inversion. On cooling, however, the crystal undergoes a phase transition at about 194 K, below which the molecule is twisted though it still occupies the inversion center.[9] The space group of the low temperature phase is $P\bar{1}$. Similar phase transitions (twist transitions) have been observed in the related substances, so-called poly(*p*-phenylene)s, i.e. in biphenyl[10-17] at 40.4 K[18-20] and in *p*-quaterphenyl[21,22] at 233.0 K.[23]

Many experimental works which made use of optical[24-31] and other techniques[32-40] have revealed that the transition of *p*-terphenyl is continuous or very-nearly continuous under the normal pressure. Under high pressures ($\gtrsim 10^8$ Pa), the transition has been reported discontinuous.[19,31] Critical exponents for some physical properties under the normal pressure have been reported as β=0.15[41] and ν=0.12.[42] These values can be related to a two-dimensional Ising model. The two-dimensionality of the interaction has been supported by neutron[43,44] and NMR[45] experiments.

Baudour et al.[7] refined the crystal structure at room temperature on the assumption that the room temperature phase was a disordered one. They have obtained a doubly peaked electron density diagram for the central phenyl ring, which strongly suggests an order-disorder nature of the transition and is consistent with the failure in search for soft-modes.[25,26] Dynamical aspects of the transition have been investigated by using neutron scattering[41,43,44,46,47] and NMR,[45,48-51] and thereby the critical phenomenon, the critical slowing down of the order parameter fluctuation, was found, which also implied an order-disorder nature of the transition.

It is interesting to note that the pressure dependence of the transition temperature is negative,[29,31] which fact also suggests that the transition is related to a subtle balance between intra- and intermolecular interactions because the intermolecular interaction, which prefers a planar conformation, is more affected by compression than the intramolecular interaction.

A theoretical work by Ramdas and Thomas[52] predicted the existence of another unknown phase on the basis of calculation of static lattice energies. Raich and Bernstein[53] theoretically confirmed an order-disorder nature of the transition through calculation of generalized susceptibility of twisting motion within one-particle scheme.

Although extensive investigations have been carried out on the twist transitions of poly(*p*-phenylene)s and many interesting features were revealed, no systematic study had been reported on thermodynamics of the transitions when we began thermodynamic investigations on biphenyl and related substances[18-20,23,54-60] in an attempt toward a unified understanding of the twist transitions of poly(*p*-phenylene)s. After completion of the study presented here, the results of precision heat capacity measurements on nonlabelled *p*-terphenyl were reported by Chang.[40] Because we measured also on *p*-terphenyl-d_{14} for which there had been no precision thermodynamic data reported, we thought it deserves publication. To provide a consistent set of data from the same calorimeter, we will record the heat capacity values of nonlabelled *p*-terphenyl as well as those of *p*-terphenyl-d_{14}.

Experimental

p-Terphenyl was purchased from Nakarai Chemicals, Ltd. and purified by the method of fractional sublimation in vacuum at about 400 K. The purity of the sublimed specimen was better than 99.9 moles per cent as confirmed by gas chromatography. A part of the sublimed specimen

† Contribution No. 143 from Chemical Thermodynamics Laboratory, Faculty of Science, Osaka University.

was used for adiabatic calorimetry without any further treatment; it weighed 21.0701 g (0.091488 mol) in vacuum. The rest of the sublimed specimen was melted under a helium atmosphere (10^5 Pa), gradually cooled down to room temperature for recrystallization, and pulverized gently. The heat capacity of the melt-pulverized sample was also measured; its mass was 15.2290 g (0.066124 mol). Each sample was loaded into a gold-plated copper calorimeter vessel, which was sealed after adding some helium gas (7 kPa at room temperature) to aid thermal uniformity of the vessel. The contribution of the helium gas was negligibly small in comparison with both the sample and the total heat capacities. The as-sublimed sample contributed 64 per cent at 10 K to the total heat capacity including that of the calorimeter vessel; the contribution decreased to 40 per cent at 100 K and then increased to 54 per cent at 300 K as temperature rose.

p-Terphenyl-d_{14} (nominal isotope purity of 98 per cent, Merck Sharp & Dohme Canada, Ltd.) was purified by fractional sublimation in vacuum at about 400 K. The sublimed specimen was melted under a helium atmosphere (10^5 Pa) and cooled gradually down to room temperature for recrystallization. The specimen was then pulverized gently for the ease of loading it into the calorimeter vessel. The chemical and the isotope purities of the specimen were better than 99.9 moles per cent as confirmed by gas chromatography and 98 per cent by high-resolution NMR, respectively. The powdered specimen (8.7131 g, 0.035652 mol) was loaded into the same calorimeter vessel and treated in the same way as for *p*-terphenyl. The contribution of the sample to the total heat capacity was 51 per cent at 10 K, 27 per cent at 100 K and 42 per cent at 300 K.

The working thermometers attached to the calorimeter vessel were a platinum (model 8164, Leeds & Northrup Co.) and a germanium (model CR-1000, CryoCal Inc.) resistance thermometers. Their temperature scales are based on the IPTS-68, helium gas thermometry and the 1958 ^{4}He vapor pressure scale. The apparatus and the operation of the adiabatic calorimetry were the same as described elsewhere.[58]

Results and Discussion

Heat Capacities and Thermodynamic Functions.

The heat capacity measurements were made between 3 and 300 K. The primary data are tabulated in Table 1 for *p*-terphenyl and Table 2 for *p*-terphenyl-d_{14} in chronological sequence and both are plotted in Fig. 1, where data of the *p*-terphenyl specimen that was sublimed and melted are not included. Curvature corrections were not made. After each energy input was over, thermal equilibrium within the calorimeter vessel was attained in 2 min below 20 K. As temperature rose, the time needed for equilibration gradually increased to 10 min at 80 K and 20 min just below the transition temperature, and it abruptly decreased to 10 min above the transition.

As the difference in sample preparation might cause differences in thermodynamic properties especially at the phase transition, the heat capacities of the as-sublimed *p*-terphenyl sample was compared with

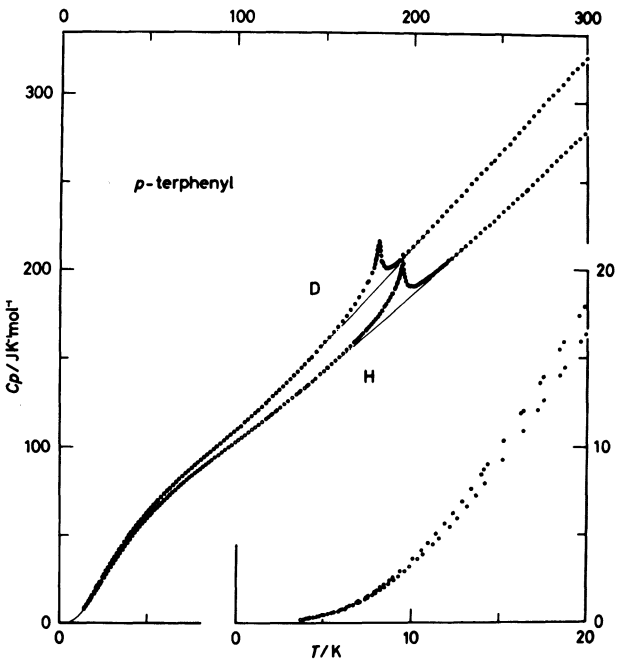

Fig. 1. Measured molar heat capacities of *p*-terphenyl (○) and *p*-terphenyl-d_{14} (●).

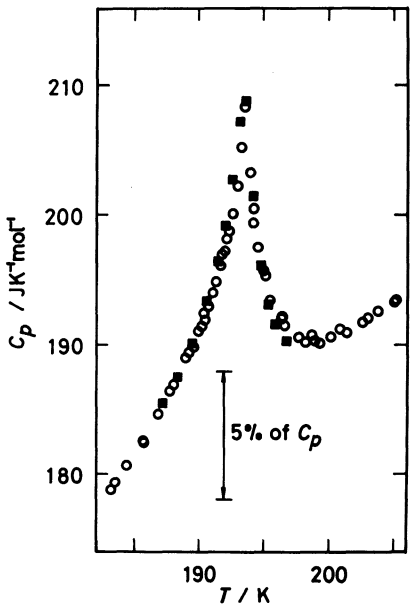

Fig. 2. Comparison of the anomalies due to the twist transition of the as-sublimed (○) and the sublimed-melted (■) *p*-terphenyl samples.

those of the melt-pulverized sample as shown in Fig. 2. The fact that there is no apparent difference rules out any possibilities of the formation of metastable phases and/or difference in crystallinity.

Figure 3 shows deviations of the present and Chang's[40] data from the smooth heat capacities determined from the present *p*-terphenyl results. The present results are systematically smaller by ca. 0.2 per cent than Chang's data in other than the transition region above 20 K.

Table 1. Measured Molar Heat Capacities of *p*-Terphenyl

T	$C_{p,m}$	T	$C_{p,m}$	T	$C_{p,m}$	T	$C_{p,m}$	T	$C_{p,m}$
K	$J K^{-1} mol^{-1}$	K	$J K^{-1} mol^{-1}$	K	$J K^{-1} mol^{-1}$	K	$J K^{-1} mol^{-1}$	K	$J K^{-1} mol^{-1}$
as-sublimed sample		248.401	230.28	192.042	197.26	5.164	0.449	Series 25	
Series 1		251.110	233.11	192.358	198.77	5.549	0.549	56.689	67.044
118.932	117.87	253.820	235.56	192.677	200.09	5.928	0.673	58.033	68.438
120.626	119.82	256.511	238.22	192.996	202.20	6.293	0.809	Series 26	
122.532	120.82	259.160	240.71	193.313	205.17	6.650	0.946	189.034	188.97
124.595	122.44	261.845	242.95	193.628	208.36	7.014	1.109	190.434	192.46
126.794	124.29	264.277	245.37	193.943	203.25	7.397	1.301	191.770	196.96
129.081	126.00	Series 7		194.259	199.35	7.811	1.548	192.414	200.65
Series 2		265.118	246.09	194.575	197.55	8.258	1.840	192.478	200.89
129.181	125.88	267.871	248.87	194.892	195.77	8.741	2.181	192.562	201.15
131.472	127.80	270.598	251.68	Series 13		9.279	2.619	192.671	201.04
133.763	129.71	273.358	254.20	195.549	193.55	9.897	3.168	192.805	201.83
136.027	131.62	276.152	256.83	196.588	191.55	10.646	3.870	192.962	203.13
138.259	133.43	278.924	259.69	197.719	190.65	11.555	4.794	193.144	204.02
140.461	135.17	281.670	262.39	198.921	190.32	12.590	5.928	193.342	206.54
142.655	136.94	284.395	264.95	200.148	190.59	13.663	7.239	193.521	209.80
144.841	138.86	287.157	267.44	201.373	190.94	Series 19		193.672	210.71
146.986	140.98	289.959	270.62	202.595	191.68	6.720	0.989	193.810	207.64
149.059	142.65	292.736	273.02	203.813	192.58	7.111	1.174	193.935	205.46
151.056	144.76	295.492	275.42	205.026	193.29	7.528	1.391	194.051	203.97
152.989	145.90	298.228	278.16	206.237	194.11	7.983	1.669	194.163	202.47
Series 3		Series 8		207.456	194.99	8.478	2.003	194.279	201.77
132.987	128.86	84.253	90.983	208.685	195.91	9.019	2.419	194.405	200.39
135.299	130.88	86.121	92.552	209.909	196.80	9.631	2.941	Series 27	
137.593	132.92	87.982	94.001	211.129	197.80	10.358	3.622	195.123	195.31
139.847	134.66	89.838	95.456	212.344	198.78	11.218	4.456	196.436	192.09
142.087	136.67	91.722	96.907	213.555	199.73	12.184	5.471	Series 28	
144.356	138.52	93.632	98.347	214.776	200.78	13.175	6.623	188.569	187.35
146.611	140.57	95.562	99.842	216.005	201.78	Series 20		189.662	189.94
148.884	142.43	97.461	101.15	217.224	202.87	17.163	12.094	198.214	190.15
151.173	144.51	99.337	102.73	218.437	203.77	18.440	14.041	199.291	190.12
153.429	146.53	101.230	104.07	219.651	205.10	19.654	15.946	sublimed and melted sample	
155.620	148.53	103.079	105.45	Series 14		20.789	17.740		
157.745	150.60	Series 9		51.458	61.431	21.939	19.591	Series 29	
Series 4		104.949	106.85	53.397	63.571	23.105	21.503	187.284	185.49
159.931	152.59	106.850	108.42	54.967	65.232	24.292	23.462	188.348	187.52
162.093	154.73	108.727	109.90	56.523	66.812	Series 21		189.461	190.24
164.230	156.87	110.581	111.27	58.044	68.382	14.022	7.737	190.605	193.43
166.387	159.03	112.459	112.70	59.573	69.909	15.155	9.246	191.471	196.46
168.563	161.29	114.364	114.18	61.113	71.344	16.338	10.899	192.043	199.33
170.717	163.60	116.248	115.66	62.648	72.843	17.524	12.633	192.598	202.73
172.854	165.87	118.112	117.18	64.185	74.331	18.724	14.478	193.136	207.25
174.974	168.29	119.971	118.65	65.742	75.647	19.920	16.375	193.669	208.85
177.114	170.75	Series 10		67.319	77.107	21.113	18.250	194.206	201.47
179.273	173.41	116.646	115.94	68.905	78.503	22.311	20.199	194.752	196.11
181.410	176.38	119.536	118.27	70.475	79.884	23.517	22.186	195.306	193.07
183.520	179.37	121.996	120.12	72.029	81.161	24.732	24.183	195.859	191.58
185.649	182.59	Series 11		73.594	82.532	Series 22		196.693	190.35
187.795	186.42	167.071	159.49	75.145	83.762	21.983	19.641	Series 30	
189.955	191.09	168.073	160.68	76.688	85.031	23.168	21.574	189.949	191.44
192.121	198.23	169.090	161.76	78.224	86.303	24.373	23.544	191.053	195.01
194.313	200.52	170.141	162.87	79.754	87.473	25.599	25.537	192.087	199.51
196.515	192.22	171.228	163.91	81.303	88.765	Series 23		192.621	201.61
198.679	190.77	172.355	165.23	82.847	89.977	26.845	27.628	192.721	202.54
200.840	191.22	173.522	166.52	84.388	91.148	28.106	29.627	192.829	203.63
202.991	192.04	174.730	167.98	Series 15		29.383	31.666	192.940	204.74
205.132	193.46	175.957	169.33	3.732	0.184	30.671	33.715	193.052	205.69
207.263	194.91	177.177	170.79	3.873	0.239	31.965	35.765	193.164	206.94
209.394	196.46	178.394	172.23	3.991	0.268	33.266	37.775	193.275	208.30
Series 5		179.607	173.66	Series 16		34.590	39.748	193.387	209.50
210.577	197.08	180.807	175.25	4.627	0.321	35.929	41.715	193.501	209.35
213.355	199.13	182.015	176.98	5.073	0.425	37.298	43.709	193.614	209.55
		183.231	178.75	5.491	0.536	38.699	45.627	193.726	208.13

Table 1. (Continued)

T	$C_{p,m}$	T	$C_{p,m}$	T	$C_{p,m}$	T	$C_{p,m}$	T	$C_{p,m}$
K	J K^{-1} mol^{-1}	K	J K^{-1} mol^{-1}	K	J K^{-1} mol^{-1}	K	J K^{-1} mol^{-1}	K	J K^{-1} mol^{-1}
216.112	201.75	184.437	180.65	5.882	0.635	40.101	47.563	193.839	206.00
218.845	204.04	185.646	182.52	6.285	0.759	41.509	49.465	193.950	204.54
221.560	206.31	186.861	184.59	Series 17		42.928	51.319	194.063	202.34
224.244	208.60	188.067	186.85	3843	0.207	44.344	53.107	194.174	201.13
226.936	211.01	189.277	189.40	4.079	0.222	45.747	54.813	194.285	199.73
229.619	213.39	Series 12		4.436	0.287	47.109	56.480	194.396	198.26
232.307	216.14	190.003	190.22	4.838	0.369	48.460	58.096	194.506	197.15
235.026	218.32	190.250	191.46	5.235	0.467	49.838	59.713	195.088	194.20
237.725	220.77	190.520	191.88	5.610	0.576	51.207	61.229		
240.404	223.51	190.806	192.90	Series 18		Series 24			
Series 6		191.106	193.95	4.077	0.221	52.567	62.714		
243.063	225.35	191.415	194.89	4.422	0.278	53.948	64.261		
245.714	227.74	191.726	196.09	4.790	0.363	55.328	65.649		

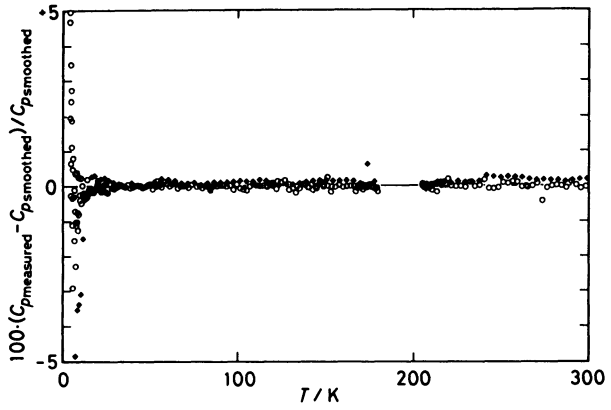

Fig. 3. Deviations of the measured values from the smooth curve determined from the present data for *p*-terphenyl; O, present work; ◆, Chang.[40]

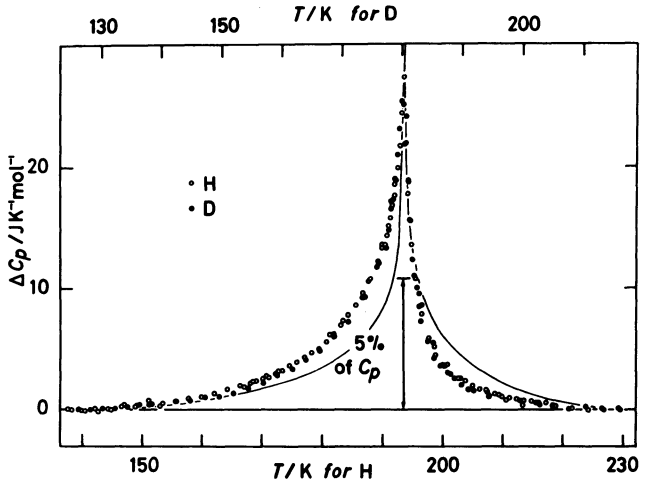

Fig. 4. Excess heat capacities due to the twist transition of *p*-terphenyl (O) and *p*-terphnyl-d_{14} (●).

Some thermodynamic quantities calculated from the present results are given at rounded temperatures in Tables 3 and 4, where small contributions below 4 K were estimated by extrapolating the heat capacity curve from the high temperature side smoothly.

Anomaly Due to Phase Transition. As clearly seen in Fig. 1, the twist transition is observed as a λ-shaped anomaly with a maximum at (193.5±0.1) K for *p*-terphenyl and (180.3±0.1) K for *p*-terphenyl-d_{14}. The transition temperature of the H compound reported by Chang[40] (193.55 K) agrees well with our result. The general shape of the anomaly is also in good agreement. The C_p maximum determined by Cailleau and Dworkin[39] occurred at 193.33 K, whereas they gave 191.0 K from DSC experiment. Cailleau and Dworkin also reported the transition temperature of the D compound as 178.8 K from DSC. In spite of sharp rise in heat capacity, no latent heat was detected in agreement with the results reported by Cailleau and Dworkin,[39] and Chang.[40] By assuming the normal portions of heat capacity as shown by the solid lines in Fig. 1, the excess parts were separated. This can be seen in Fig. 4 and the anomaly ranges from 145 K to 225 K (*p*-terphenyl) and 130 K to 210 K (*p*-terphenyl-d_{14}). The values of the enthalpies and the entropies of transition obtained by graphical integration are given in Table 5 and compared with the literature values.[39,40] Small differences between ours and those reported by Chang[40] are mainly due to the difference in estimation of the normal portion of heat capacity. As the estimation of the excess parts is more or less artificial in cases of structural phase transitions, it is considered that these values are in reasonable agreement. Thus, the entropy of transition of *p*-terphenyl is much larger than that of biphenyl (0.129J·K^{-1}·mol^{-1})[18-20] which undergoes a displacive type of transition. This fact is consistent with an order-disorder nature of the transition of *p*-terphenyl. The detailed comparison of the properties of the twist transitions of biphenyl, *p*-terphenyl, and *p*-quaterphenyl was given in a previous paper.[23]

The critical exponent α for heat capacity was determined by plotting the excess heat capacities

$$\Delta C_p^{\alpha} | T - T_c |^{-\alpha}$$

Table 2. Measured Molar Heat Capacities of *p*-Terphenyl-d_{14}

T	$C_{p,m}$	T	$C_{p,m}$	T	$C_{p,m}$	T	$C_{p,m}$	T	$C_{p,m}$
K	$J K^{-1} mol^{-1}$	K	$J K^{-1} mol^{-1}$	K	$J K^{-1} mol^{-1}$	K	$J K^{-1} mol^{-1}$	K	$J K^{-1} mol^{-1}$
Series 1		Series 4		83.618	95.826	4.519	0.296	24.063	25.303
142.267	150.48	279.816	299.94	85.388	97.317	4.839	0.359	25.287	27.439
144.794	153.56	282.655	302.99	87.152	98.842	5.192	0.463	26.497	29.520
147.334	156.47	285.502	306.32	88.910	100.47	5.558	0.565	27.712	31.555
149.665	158.99	288.352	309.64	90.677	101.93	5.936	0.714	28.927	33.609
152.056	161.76	291.174	313.32	Series 8		6.342	0.869	30.140	35.636
154.573	164.81	294.009	315.59	182.115	203.82	6.753	1.068	31.362	37.661
157.063	167.87	296.862	318.24	183.211	201.27	7.168	1.268	32.617	39.710
159.418	170.97	299.698	321.16	184.327	200.84	7.549	1.502	33.940	41.746
161.791	174.03	Series 5		185.440	200.68	Series 13		35.319	43.847
164.181	177.40	91.195	102.03	186.551	201.29	6.149	0.830	36.883	46.212
166.546	180.78	93.075	103.75	187.659	201.91	6.573	0.990	38.322	48.250
168.889	184.39	94.948	105.45	188.782	202.69	7.004	1.244	39.533	49.948
171.228	188.13	96.816	107.06	189.925	203.43	7.442	1.421	40.866	51.805
173.583	192.67	98.711	108.73	191.065	204.32	7.893	1.736	42.205	53.627
175.931	197.74	100.633	110.38	Series 9		Series 14		43.587	55.481
178.266	205.75	102.585	111.84	173.981	193.16	7.378	1.377	45.003	57.230
180.605	213.00	104.553	114.02	176.192	198.38	7.799	1.663	46.463	59.014
182.942	203.25	106.523	115.67	177.476	201.00	8.248	1.999	47.950	60.875
185.250	201.87	108.483	117.52	177.849	202.93	8.757	2.402	49.351	62.591
187.531	202.89	110.431	119.24	178.215	205.09	9.360	2.931	50.676	64.101
Series 2		112.369	121.05	178.579	206.24	10.069	3.632	52.022	65.602
187.146	201.92	114.299	122.72	178.942	208.32	10.924	4.532	53.393	67.179
189.571	203.70	116.236	124.58	179.304	210.69	11.869	5.644	54.795	68.648
192.027	205.25	Series 6		179.663	213.16	12.858	6.878	Series 20	
194.514	207.51	116.432	125.01	180.022	215.83	13.939	8.403	177.334	200.67
197.057	210.10	118.359	126.66	180.379	215.97	Series 15		178.121	201.93
199.680	212.87	120.292	128.72	180.737	215.33	8.032	1.844	178.246	202.69
202.363	215.69	122.251	130.46	181.096	210.46	8.463	2.179	178.368	201.06
205.077	218.47	124.224	132.27	181.457	207.66	8.964	2.588	178.496	202.09
207.832	221.30	126.209	134.21	181.819	204.79	Series 16		178.627	202.17
210.595	224.50	128.206	136.13	182.183	203.68	10.569	4.126	178.760	204.15
213.330	227.39	130.215	138.23	182.548	203.27	11.381	5.073	178.896	204.23
216.071	231.42	132.287	140.32	182.914	202.14	12.342	6.238	179.032	204.44
218.647	233.40	134.353	142.47	184.172	201.70	13.372	7.594	179.166	205.76
221.162	236.11	136.368	144.67	Series 10		Series 17		179.301	207.58
223.936	238.89	138.399	146.73	3.955	0.205	14.286	9.005	179.434	209.39
226.839	242.18	140.446	148.97	4.233	0.267	15.205	10.365	179.567	210.85
229.707	245.29	142.509	151.18	4.599	0.316	16.317	12.033	179.700	210.80
232.554	249.10	144.589	153.51	4.962	0.401	17.483	13.932	179.833	211.06
235.392	251.79	Series 7		5.325	0.518	18.657	15.896	179.967	211.99
238.209	255.00	55.803	69.701	5.702	0.639	19.863	17.955	180.099	211.82
241.003	257.48	57.703	71.753	6.096	0.783	21.130	21.131	180.231	212.56
243.829	260.69	59.411	73.517	6.501	0.954	Series 18		180.364	213.68
Series 3		61.058	75.264	6.899	1.152	14.082	8.687	180.497	211.43
245.835	262.31	62.739	76.782	Series 11		15.169	10.325	180.630	211.20
248.683	265.60	64.447	78.554	3.921	0.186	16.215	11.889	180.763	209.40
251.509	268.74	66.162	80.104	4.245	0.250	17.287	13.602	180.896	208.35
254.342	271.74	67.914	81.788	4.604	0.319	18.402	15.467	181.030	206.38
257.182	274.92	69.660	83.441	4.965	0.431	19.544	17.417	181.164	205.34
260.001	278.28	71.408	85.110	5.283	0.490	20.739	19.469	181.299	203.20
262.830	281.33	73.158	86.590	5.624	0.601	22.015	21.650	181.433	202.35
265.691	284.55	74.912	88.235	5.988	0.729	23.289	23.931		
268.533	287.87	76.648	89.721	Series 12		24.493	26.040		
271.358	291.07	78.371	91.207	3.789	0.145	Series 19			
274.188	294.01	80.105	92.711	3.981	0.191	21.611	20.968		
276.997	297.81	81.853	94.290	4.219	0.240	22.837	23.127		

Table 3. Molar Thermodynamic Functions of *p*-Terphenyl

T	$C_{p,m}$	$[H^\circ_m(T)-H^\circ_m(0)]/T$	$S^\circ_m(T)-S^\circ_m(0)$	$-[G^\circ_m(T)-H^\circ_m(0)]/T$
K	J K^{-1} mol^{-1}	J K^{-1} mol^{-1}	J K^{-1} mol^{-1}	J K^{-1} mol^{-1}
5	0.392	0.101	0.131	0.030
10	3.27	0.82	1.08	0.27
20	16.49	5.07	7.01	1.95
30	32.67	11.57	16.75	5.19
40	47.44	18.75	28.23	9.49
50	59.86	25.76	40.19	14.44
60	70.28	32.33	52.05	19.73
70	79.46	38.43	63.59	25.17
80	87.72	44.08	74.74	30.67
90	95.57	49.37	85.53	36.17
100	103.19	54.37	96.00	41.64
110	110.81	59.15	106.19	47.05
120	118.63	63.78	116.16	52.39
130	126.68	68.31	125.98	57.68
140	134.84	72.77	135.66	62.90
150	143.45	77.19	145.26	68.08
160	152.70	81.62	154.81	73.20
170	162.77	86.09	164.36	78.28
180	174.45	90.66	173.98	83.33
190	191.06	95.47	183.81	88.35
200	190.33	100.43	193.81	93.39
210	196.86	104.86	203.24	98.40
220	204.98	109.22	212.58	103.37
230	213.81	113.57	221.88	108.32
240	222.75	117.93	231.17	113.25
250	231.85	122.31	240.45	118.16
260	241.23	126.70	249.72	123.03
270	250.91	131.12	259.01	127.90
280	260.71	135.58	268.31	132.74
290	270.30	140.06	277.63	137.58
300	279.90	144.56	286.95	142.40
298.15	278.12	143.72	285.23	141.52

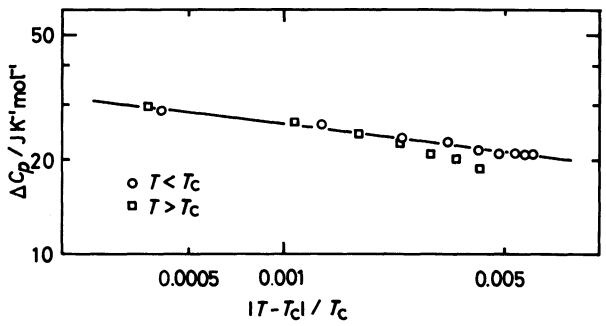

Fig. 5. Determination of the critical exponent α.

measured in series 26 in Table 1 as shown in Fig. 5. The temperature interval between adjacent points is about 0.1 K. The same value, $\alpha=0.13$, was obtained below and above the transition. This value is more like that of three-dimensional Ising model, and the positive sign of the exponent should result in an infinite heat capacity at the transition point. However, the measured heat capacity is finite at the transition point. Chang[40] reported an apparent rounding of the anomaly using a smaller temperature increment (0.025 K). He gave a larger α of 0.55 below the phase transition from a very detailed study close to the C_p maximum. It was not possible to obtain α for *p*-terphenyl-d_{14} because scatter of the measured points was larger.

Now, we will compare thermodynamic properties of the twist transitions in crystalline *p*-terphenyl and *p*-terphenyl-d_{14}. The shapes of the anomalies and the values of the entropies of transition indicate that the two compounds undergo the transition of the same mechanism and therefore the same model should apply. On the other hand, the transition temperature lowers on deuteration by about 13 K. The lowering of the transition temperature on deuteration also occurs in biphenyl.[18-20,58] Since the inter- and the intramolecular interactions are expected almost the same in the crystals of hydrogenated and deuterated compounds, these isotope effects reflect the roles of the molecular mass and/or moment of inertia in the twist transition though Raich and Bernstein[53] ruled out such a dynamical origin of the isotope effect. It is noteworthy that *p*-terphenyl-2,2″,3,3″,4,4″,5,5″,6,6″-d_{10} (C_6D_5–C_6H_4–C_6D_5) shows the twist transition at an intermediate temperature, 185.3 K.[47] Relative importance of the moment of inertia and the molecular mass in the mechanism of the transition will be experimentally demonstrated if one performs a study on

Table 4. Molar Thermodynamic Functions of *p*-Terphenyl-d_{14}

T	$C_{p,m}$	$[H^\circ_m(T)-H^\circ_m(0)]/T$	$S^\circ_m(T)-S^\circ_m(0)$	$-[G^\circ_m(T)-H^\circ_m(0)]/T$
K	J K^{-1} mol^{-1}	J K^{-1} mol^{-1}	J K^{-1} mol^{-1}	J K^{-1} mol^{-1}
5	0.421	0.109	0.142	0.033
10	3.56	0.89	1.17	0.28
20	18.19	5.59	7.71	2.12
30	35.41	12.68	18.37	5.68
40	50.64	20.32	30.69	10.38
50	63.30	27.68	43.39	15.71
60	74.10	34.53	55.91	21.37
70	83.77	40.89	68.09	27.18
80	92.67	46.81	79.84	33.03
90	101.22	52.39	91.25	38.87
100	109.83	57.69	102.36	44.66
110	118.88	62.85	113.25	50.40
120	128.26	67.90	123.99	56.09
130	137.97	72.92	134.64	61.72
140	148.43	77.94	145.24	67.31
150	159.32	82.99	155.85	72.86
160	171.76	88.14	166.52	78.38
170	185.90	93.46	177.34	83.88
180	215.90	99.21	188.59	89.38
190	203.50	104.70	199.60	94.90
200	213.19	109.87	210.27	100.40
210	223.79	115.04	220.93	105.98
220	234.82	120.24	231.59	111.36
230	245.72	125.46	242.27	116.82
240	256.22	130.69	252.95	122.27
250	266.93	135.92	263.63	127.71
260	278.16	141.17	274.31	133.14
270	289.48	146.46	285.03	138.57
280	300.54	151.76	295.75	143.99
290	311.27	157.08	306.49	149.41
300	321.55	162.39	317.22	154.82
298.15	319.66	161.41	315.23	153.82

Table 5. Properties of the Twist Transitions of *p*-Terphenyl and *p*-Terphenyl-d_{14}

		This work	Chang[40]	Dworkin and Cailleau[39]
p-Terphenyl	T_{trs}/K	193.5±0.1	193.55	193.33
	region/K	145—225	140—240	(175—200)[a]
	$\Delta_{trs}H$/J·mol^{-1}	304±20	334	
	$\Delta_{trs}S$/J·K^{-1}·mol^{-1}	1.63±0.10	1.80	0.49
p-Terphenyl-d_{14}	T_{trs}/K	180.3±0.1		178.8[b]
	region/K	130—210		
	$\Delta_{trs}H$/J·mol^{-1}	288±20		
	$\Delta_{trs}S$/J·K^{-1}·mol^{-1}	1.63±0.10		1.08[b]

a) Read from Fig. 1 of Ref. 39. b) Determined by DSC.

p-terphenyl-4,4″-d_2.

Although Chen et al.[38] suggested that there is another phase transition at about 8 K based from their EPR experiments, any anomalous behavior was not observed in the present experiments.

Anisotropy of Interaction The examination of crystal structures of poly(*p*-phenylene)s makes us suspect that the interaction within the ab plane (a, b, and c refer, hereafter, to the crystal axes of the room temperature phase) is much stronger than in the direction of the c axis because the nearest neighbor distance is much shorter in the ab plane than that along the c axis. Furthermore, in view of the order-disorder mechanism, it is also expected that inter-"spin" interaction, i.e. a part of the intermolecular interaction which depends on molecular twisting is much stronger within the ab plane than along the c axis since the interatomic distance between two neighboring molecules in the c direction changes little upon twisting of one of them. Indeed, two-dimensionality of interaction has been reported experimentally.[43–45]

In order to see the anisotropic interaction, we now examine the low temperature ordered structure.[9] The

structure viewed along the c axis is schematically shown in Fig. 6, where Roman numerals distinguish translationally inequivalent molecules. The solid line represents the triclinic unit cell of the low-temperature phase and the broken line the monoclinic unit cell of the room-temperature phase. All of the molecules shown there lie at the same height. Since the "spin" in this case corresponds to twisting of the central phenyl ring with respect to the outer rings, the atomic position of "wrong" molecules were determined from those of "right" molecules which are known by experiment.[9] The intermolecular interactions were then calculated assuming that it may be expressed by the sum of interatomic potentials of Buckingham type.[60] Summation was made over all the atom pairs between the two adjacent molecules under consideration.

The calculated intermolecular and inter-"spin" interactions are summarized in Table 6, where the inter-"spin" interaction energy J is defined by

$$J = \frac{1}{2}(E_{r-r} + E_{w-w}) - \frac{1}{2}(E_{r-w} + E_{w-r}).$$

It is evident that interactions within the ab plane are much stronger than those along the c axis. Thus, a two-dimensional Ising model will apply to the twist transition of *p*-terphenyl at least in the first approximation. Indeed, the experimental excess heat capacity is well reproduced with a two-dimensional Ising mdel as shown in Fig. 4.

It is well-known that the heat capacity of any two dimensional Ising model diverges as $\ln|T-T_c|$ at T_c and shows the critical exponent $\alpha=0$. However, the experimental value determined in this study is not 0 but 0.13. However, the discrepancy is not crucial because the exact formula of the heat capacity gives a slope of about 0.1 at $|T-T_c|/T_c \simeq 0.001$, where the experiments were done.

Figure 7 shows the calculated heat capacity of, for

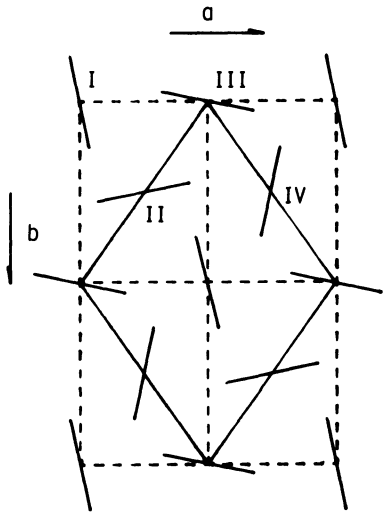

Fig. 6. Crystal structure of the low temperature phase viewed along the c axis (schematic). Broken line represents the unit cell of the room temperature phase.

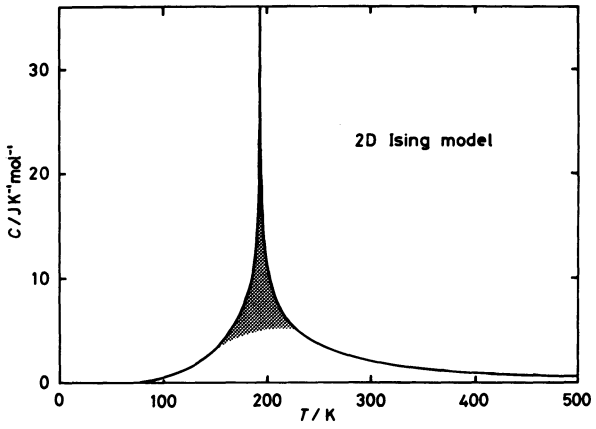

Fig. 7. Calculated heat capacity of the two-dimensional square lattice of Ising model with a critical temperature of 193.5 K.

Table 6. Calculated Inter-"spin" Interaction Energies within the ab Plane (upper) and along the c Axis (Lower)
r, "right" molecule; w, "wrong" molecule
$J=\frac{1}{2}(E_{r-r}+E_{w-w}) - \frac{1}{2}(E_{r-w}+E_{w-r})$

	E_{r-r}	E_{r-w}	E_{w-r}	E_{w-w}	J
	kJ·mol^{-1}	kJ·mol^{-1}	kJ·mol^{-1}	kJ·mol^{-1}	kJ·mol^{-1}
I-II	−39.54	−39.46	−39.72	−39.75	−0.06
II-III	−39.98	−39.91	−37.64	−39.21	−1.17
III-IV	−38.75	−36.86	−36.59	−37.97	−1.64
IV-I	−39.80	−38.60	−39.00	−38.89	−0.55
I-III	−28.59	−22.72	−13.90	−28.55	−10.26
II-IV	−28.28	−20.65	−25.43	−28.32	−5.26
I-I	−7.25	−7.34	−7.34	−7.34	0.00
II-II	−7.28	−7.14	−7.14	−6.97	0.02
III-III	−7.40	−7.10	−7.10	−6.76	0.02
IV-IV	−7.16	−7.13	−7.13	−7.06	0.02

simplicity, the two-dimensional square lattice of Ising model[61] with the critical temperature of 193.5 K (J=709 J·mol^{-1}). There exist large tails on both the lower and the higher temperature sides of the transition. Remember that the experimental excess heat capacity was separated by drawing the smooth interpolating curve. For the sake of consistent comparison, therefore, the theoretical "excess" heat capacity should be separated also in the same manner as the experimental. This was done in the transition region determined experimentally (145 K to 225 K). The "excess part" is shaded in Fig. 7 and compared with the experimental one in Fig. 4. While the general agreement between the calculated and experimental curves in Fig. 4 shows that the transition may be approximated by a two-dimensional order-disorder model, discrepancies at the tail parts indicates that there is room for improvement in the model; extending the range of interaction beyond the nearest neighbors and/or introducing a small contribution of the third dimension.

It is noted that the ideal value of entropy of transition, Rln2, is obtained only when one integrates C/T between zero and high-temperature limits. This will be one of the reasons why the entropy of transition is smaller than Rln2.

Finally, a comment is in order about the change in the nature of the twist transitions of poly(*p*-phenylene)s from a displacive phase transition in crystalline biphenyl to order-disorder transitions in *p*-terphenyl and in *p*-quaterphenyl. In the case of biphenyl, the substitution of *p* and *p'* hydrogens with fluorine atoms[56,59] or hydroxyl groups[57] mainly modifies the intramolecular potential for the twisting motion and the twist transition disappears owing to the stabilization of the planar conformation that favors greater π-conjugation. This suggests that the twist transition of *p*-terphenyl may change its nature from an order-disorder type to a displacive type upon such substitutions. Thus, it is interesting to investigate the properties of suitably substituted *p*-terphenyls in order to elucidate the nature of displacive and order-disorder types of phase transitions.

References

1) J. Dale, *Acta Chem. Scand.*, **11**, 640 (1957).
2) H. Suzuki, *Bull. Chem. Soc. Jpn.*, **33**, 109 (1960).
3) S. Hino, K. Seki, and H. Inokuchi, *Chem. Phys. Lett.*, **36**, 335 (1976).
4) A. J. Grumadas, D. P. Poshkus, and A. V. Kiselev, *J. Chem. Soc., Faraday Trans. 2*, **78**, 2013 (1982).
5) H. M. Rietveld, E. N. Maslen, and C. J. B. Clews, *Acta Crystallogr., Sect. B*, **26**, 693 (1970).
6) J. L. Baudour, *Acta Crystallogr., Sect. B*, **28**, 1649 (1972).
7) J. L. Baudour, H. Cailleau, and W. B. Yelon, *Acta Crystallogr., Sect. B*, **33**, 1773 (1977).
8) J. L. Baudour, L. Toupet, Y. Delugeard, and S. Ghemid, *Acta Crystallogr., Sect. C*, **42**, 1211 (1987).
9) J. L. Baudour, Y. Delugeard, and H. Cailleau, *Acta Crystallogr., Sect. B*, **32**, 150 (1976).
10) J. Trotter, *Acta Crystallogr.*, **14**, 1135 (1961).
11) G. B. Robertson, *Nature (London)*, **191**, 593 (1961).
12) A. Hargreaves and S. H. Rizvi, *Acta Crystallogr.*, **15**, 365 (1962).
13) V. M. Kozhin and K. V. Mirskaya, *Sov. Phys. Crystallogr.*, **14**, 938 (1970).
14) G. P. Charboneau and Y. Delugeard, *Acta Crystallogr., Sect. B*, **32**, 1420 (1976).
15) G. P. Charboneau and Y. Delugeard, *Acta Crystallogr., Sect. B*, **33**, 1586 (1977).
16) H. Cailleau, J. L. Baudour, and C. M. E. Zeyen, *Acta Crystallogr., Sect. B*, **35**, 426 (1979).
17) J. L. Baudour and M. Sanquer, *Acta Crystallogr., Sect. B*, **39**, 75 (1983).
18) T. Atake and H. Chihara, *Solid State Commun.*, **35**, 131 (1980).
19) T. Atake, K. Saito, and H. Chihara, *Chem. Lett.*, **1983**, 493.
20) K. Saito, T. Atake, and H. Chihara, *Bull. Chem. Soc. Jpn.*, in press.
21) Y. Delugeard, J. Desuche, and J. L. Baudour, *Acta Crystallogr., Sect. B*, **32**, 702 (1976).
22) J. L. Baudour, Y. Delugeard, and P. Rivet, *Acta Crystallogr., Sect. B*, **34**, 625 (1978).
23) K. Saito, T. Atake, and H. Chihara, *J. Chem. Thermodyn.*, **17**, 539 (1985).
24) B. Wyncke, F. Brehat, and A. Hadni, *J. Phys. (Paris)*, **38**, 1171 (1977).
25) A. Girard, H. Cailleau, Y. Marqueton, and C. Ecolivet, *Chem. Phys. Lett.*, **54**, 479 (1978).
26) B. A. Bolton and P. N. Prasad, *Chem. Phys.*, **35**, 331 (1978).
27) D. Kirin, S. L. Chaplot, G .A. Mackenzie, and G. S. Pawley, *Chem. Phys. Lett.*, **102**, 105 (1983).
28) C. Ecolivet, B. Toudic, and M. Sanquer, *J. Chem. Phys.*, **81**, 599 (1984).
29) H. Cailleau, A. Girard, J. C. Messager, Y. Delugeard, and C. Vettier, *Ferroelectrics*, **54**, 257 (1984).
30) A. Girard, M. Sanquer, and Y. Delugeard, *Chem. Phys.*, **96**, 427 (1986).
31) A. Girard, Y. Delugeard, and H. Cailleau, *J. Phys. (Paris)*, **48**, 1751 (1987).
32) J. Fünfschilling, L. Altwegg, I. Z. Granacher, M. Chabr, and D. F. Williams, *J. Chem. Phys.*, **70**, 4622 (1979).
33) J. O. Williams, *Chem. Phys. Lett.*, **42**, 171 (1976).
34) Z. Burshtein and D. F. Williams, *J. Chem. Phys.*, **68**, 983 (1978).
35) N. I. Wakayama, *Chem. Phys. Lett.*, **70**, 397 (1980).
36) N. I. Wakayama, S. Matsuzaki, and M. Mizuno, *Chem. Phys. Lett.*, **74**, 37 (1980).
37) N. I. Wakayama, S. Matsuzaki, and M. Mizuno, *Chem. Phys. Lett.*, **75**, 587 (1980).
38) M. C. Chen, A. S. Cullick, R. E. Gerkin, and A. P. Lundstedt, *Chem. Phys.*, **46**, 423 (1980).
39) H. Cailleau and A. Dworkin, *Mol. Cryst. Liq. Cryst.*, **50**, 217 (1979)
40) S. S. Chang, *J. Chem. Phys.*, **79**, 6229 (1983).
41) H. Cailleau, J. L. Baudour, A. Girard, and W. B. Yelon, *Solid State Commun.*, **20**, 577 (1976)

42) H Cailleau, J. L. Baudour, W. B. Yelon, A. Girard, Y. Delugeard, and J. Desuche, *J. Phys. (Paris), Colloq.*, **37**, C1-233 (1976).
43) R. E. Lechner, B. Toudic, and H. Cailleau, *J. Phys. C*, **17**, 405 (1984).
44) B. Toudic and R. E. Lechner, *J. Phys. C*, **17**, 5503 (1984).
45) T. Gullion M. S. Conradi, and A. Rigamonti, *Phys. Rev. B*, **31** 4388 (1985).
46) H. Cailleau, A. Heidemann, and C. M. E. Zeyen, *J. Phys. C*, **12**, L411 (1979).
47) B. Toudic, H. Cailleau, R. E. Lechner, and W. Petry, *Phys. Rev. Lett.*, **56**, 347 (1986).
48) Z. Pajak, N. Pislewski, and J. Wasicki, Proc. XI-th Sem. NMR, 190 (1980).
49) K. Kohda, N. Nakamura, and H. Chihara, *J. Phys. Soc. Jpn.*, **51**, 3936 (1982).
50) B. Toudic, J. Gallier, P. Rivet, and H. Cailleau, *Solid State Commun.*, **47**, 291 (1983).
51) T. Gullion and M. S. Conradi, *Phys. Rev. B*, **30**, 1133 (1984).
52) S. Ramdas and J. M. Thomas, *J. Chem. Soc., Faraday Trans. 2*, **72**, 1251 (1976).
53) J. C. Raich and E. R. Bernstein, *Mol. Phys.*, **53**, 597 (1984)
54) K. Saito, T. Atake, and H. Chihara, *Chem. Lett.*, **1984**, 521.
55) K. Saito, H. Chihara. T. Atake, and Y. Saito, *Jpn. J. Appl. Phys.*, **24**, Suppl. **24-2**, 838 (1985).
56) K. Saito, T. Atake, and H. Chihara, *J. Chem. Thermodyn.*, **18**, 407 (1986).
57) K. Saito, T. Atake, and H. Chihara, *Thermochim. Acta*, **109**, 45 (1986).
58) K. Saito, T. Atake, and H. Chihara, *J. Chem. Thermodyn.*, **19**, 633 (1987).
59) K. Saito. T. Atake, and H. Chihara, *Acta Crystallogr., Sect. B*, **43**, 383 (1987).
60) D. E. Williams, *J. Chem. Phys.*, **47**, 4680 (1967).
61) L. Onsager, *Phys. Rev.*, **65**, 117 (1944).